PHYSICAL REVIEW B **92**, 140201(R) (2015)

Anisotropic spin relaxation in *n*-GaAs from strong inhomogeneous hyperfine fields produced by the dynamical polarization of nuclei

N. J. Harmon,[1,*] T. A. Peterson,[2] C. C. Geppert,[2] S. J. Patel,[3] C. J. Palmstrøm,[3,4] P. A. Crowell,[2] and M. E. Flatté[1]

[1]*Department of Physics and Astronomy and Optical Science and Technology Center, University of Iowa, Iowa City, Iowa 52242, USA*

[2]*School of Physics and Astronomy, University of Minnesota, Minneapolis, Minnesota 55455, USA*

[3]*Department of Materials, University of California, Santa Barbara, California 93106, USA*

[4]*Department of Electrical and Computer Engineering, University of California, Santa Barbara, California 93106, USA*

(Received 5 May 2015; revised manuscript received 12 August 2015; published 7 October 2015)

The hyperfine field from dynamically polarized nuclei in *n*-GaAs is very spatially inhomogeneous, as the nuclear polarization process is most efficient near the randomly distributed donors. Electrons with polarized spins traversing the bulk semiconductor will experience this inhomogeneous hyperfine field as an effective fluctuating spin precession rate, and thus the spin polarization of an electron ensemble normal to the fluctuating hyperfine fields will relax. A theory of spin relaxation based on the theory of random walks is applied to such an ensemble precessing in an oblique magnetic field, and the precise form of the (unequal) longitudinal and transverse spin relaxation is analytically derived. To investigate this mechanism, electrical three-terminal Hanle measurements were performed on epitaxially grown Co_2MnSi/*n*-GaAs heterostructures fabricated into electrical spin injection devices. The proposed anisotropic spin relaxation mechanism is required to satisfactorily describe the Hanle line shapes when the applied field is oriented at large oblique angles.

DOI: 10.1103/PhysRevB.92.140201 PACS number(s): 75.40.Gb, 72.25.Dc, 85.75.−d, 61.72.S−

Introduction. The understanding of electrical injection and detection of spin in ferromagnetic/semiconductor devices has progressed significantly over the past decade [1,2]. A key obstacle for interpreting spin transport experiments near the metal-insulator transition has been the complicating presence of dynamically polarized nuclear spins [3–5]. In the process of dynamic nuclear polarization (DNP), the electron spin polarization, maintained out of equilibrium optically or electrically, is transferred to the nuclear system over long time scales via the hyperfine interaction [6–10]. The process can produce 99% polarized nuclei at room temperature in SiC and induce nuclear fields up to 5.3 T in GaAs. The nature and distribution of the electronic states control the properties of the resulting effective hyperfine fields from DNP; for instance, electron spins in itinerant states interact rapidly with a multitude of nuclei, which dilutes the effect and leads to inefficient nuclear polarization. Spins situated at impurity sites, however, interact with many fewer nuclei, which promotes a more efficient [6] DNP. At the doping levels examined here, the different donor wave functions overlap often but do not completely fill the bulk crystal, which consequently results in a high degree of nuclear field inhomogeneity (see Fig. 1) [11,12]. Previous descriptions of the spin transport dynamics in *n*-doped semiconductors with spin drift-diffusion equations [5,13–17] have neglected this essential inhomogeneity of the nuclear field.

In the past, it has been sufficient to treat the nuclear polarization as a mean field and to assume only a single spin lifetime. This has been adequate to account for the magnitudes of the hyperfine fields, although there have always been discrepancies when quantitatively modeling Hanle effect experiments. It has been impossible to model line shapes for different degrees of noncollinearity with a single spin lifetime [5]. Here, we predict a spin relaxation mechanism in semiconductors that occurs when inhomogeneous effective magnetic fields are present, such as arise from polarized nuclei. The mechanism is anisotropic since only those components of the electron spin which are normal to the effective magnetic fields relax. The requirement of the electron spin and effective magnetic field being noncollinear is met in nearly all DNP experiments since otherwise detecting the hyperfine field is difficult [8,18]. Intermediately *n*-doped GaAs, under the conditions of DNP, offers a test bed for our theory where the inhomogeneity manifests itself as a bipartite field with values $\boldsymbol{B}_0$ or $\boldsymbol{B}_0 + \boldsymbol{B}_N$, with $\boldsymbol{B}_0$ being an applied magnetic field and $\boldsymbol{B}_N$ the nuclear field induced by DNP near a donor. The anisotropy of the spin relaxation can be probed by varying the angle of applied field with respect to the direction of injected spin since the nuclear field orientation is largely determined by the applied field. We demonstrate such a system experimentally and show that measurements of the steady-state spin polarization are consistent with the devised inhomogeneity-induced anisotropic spin relaxation mechanism. The theory described in this Rapid Communication is broadly applicable to a variety of situations where the injected electron spin is noncollinear to the nuclear fields [19–22], including both via optical and electrical spin injection, and potentially even up to room temperature in semiconductors, such as SiC, where room-temperature DNP has been demonstrated [10].

Theory. The theoretical description presented herein can be understood qualitatively by examining Fig. 1, wherein the inhomogeneity of the magnetic field is represented by random placement of distortions (in red) signifying both the presence of a donor atom and a DNP-induced nuclear field. Electron spins cross between these donor regions and regions in between donors, which lack the DNP-induced nuclear field. This transit acts on the spin similarly to an effective fluctuating Zeeman field. The lower part of Fig. 1 shows how the inhomogeneity relaxes the spin; in general, the nuclear field is noncollinear with the applied field and electron spin, which causes the precession axis to stochastically modulate when the spin changes field regions. When the transit time between

*nicholas-harmon@uiowa.edu

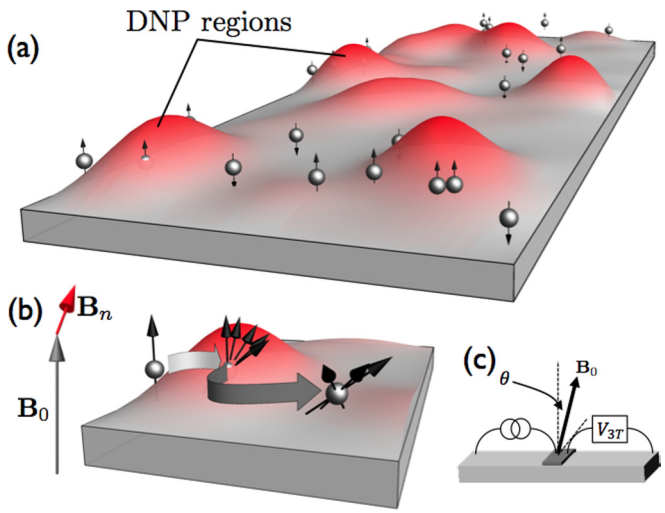

FIG. 1. (Color online) (a) Electron spins (spheres with spin vectors) in n-doped GaAs. Bumpy (red) regions depict the presence of donors and nuclear fields generated by dynamic nuclear polarization. (b) The spin rotation caused by one electron spin entering and departing a DNP region. (c) Experimental geometry, with θ being the angle between the applied field and sample normal.

these regions is much faster than the change in precession rate experienced by the spin upon transit, then the regime of spin relaxation corresponds to the motional narrowing regime. We present a general form of the theory of spin relaxation in the inhomogeneous nuclear field produced by DNP, and specifically within the motional narrowing regime we obtain compact analytic results that can be readily incorporated into spin drift-diffusion theories.

We now present a calculation of the spin relaxation of a spin ensemble, $\boldsymbol{S}$, ensuing from the aforementioned theory and assumptions. In other words, we would like to solve for the spin relaxation due to the following precession,

$$\frac{d\boldsymbol{S}(t)}{dt} = \gamma[\boldsymbol{B}_0 + \boldsymbol{B}_n(t)] \times \boldsymbol{S}(t), \tag{1}$$

where the spatial inhomogeneity of the nuclear field is written as a time-dependent nuclear field that takes on only two possible values of either $\boldsymbol{b}_n$ or 0. Since $\boldsymbol{B}_n(t)$ changes rapidly, the first approximation is to replace it with its average value, $\langle \boldsymbol{B}_n(t) \rangle = \boldsymbol{b}_n/2$, with

$$\boldsymbol{b}_n = b_{\text{nuc}}\langle \boldsymbol{I} \rangle = \frac{b_{\text{nuc}}\boldsymbol{S} \cdot (\boldsymbol{B}_0 + b_e\boldsymbol{S})}{|\boldsymbol{B}_0 + b_e\boldsymbol{S}|^2 + \xi B_\ell^2}(\boldsymbol{B}_0 + b_e\boldsymbol{S}), \tag{2}$$

where $\boldsymbol{I}$ is the nuclear spin, b_{nuc} is the Overhauser coefficient, b_e is the Knight coefficient, and $\sqrt{\xi}B_\ell$ denotes the strength of the random local field. The Knight field allows the nuclear field to be noncollinear to the applied field.

Since the average nuclear field is static, that alone will not relax the spin; temporal fluctuations around the average are required,

$$\frac{d\boldsymbol{S}(t)}{dt} = \gamma\left[\boldsymbol{B}_0 + \frac{1}{2}\boldsymbol{b}_n + \frac{1}{2}\boldsymbol{b}_n f(t)\right] \times \boldsymbol{S}(t), \tag{3}$$

where $f(t)$ is a stochastic function. $f(t)$ is equal to -1 $(+1)$ for an average time interval $1/k_0$ $(1/k_n)$, where $1/k_0$ $(1/k_n)$ is the average time the spin experiences the field $\boldsymbol{B}_0$ $(\boldsymbol{B}_0 + \boldsymbol{B}_n)$ before that field changes. We would like to find the dissipative effects from the time-dependent field so we will ignore the static applied field and average nuclear field,

$$\frac{d\boldsymbol{S}(t)}{dt} = \frac{\gamma}{2}f(t)\boldsymbol{b}_n \times \boldsymbol{S}(t) = f(t)\boldsymbol{\Omega} \cdot \boldsymbol{S}(t), \tag{4}$$

where $\boldsymbol{\Omega}(t)$ is the skew-symmetric matrix

$$\boldsymbol{\Omega} = \frac{\gamma}{2}b_n\hat{\boldsymbol{\Omega}} = \frac{\gamma}{2}b_n\begin{pmatrix} 0 & -\omega_z & \omega_y \\ \omega_z & 0 & -\omega_x \\ -\omega_y & \omega_x & 0 \end{pmatrix}$$

$$\equiv \frac{\gamma}{2}b_n\begin{pmatrix} 0 & -\cos\alpha & \sin\alpha\sin\beta \\ \cos\alpha & 0 & -\sin\alpha\cos\beta \\ -\sin\alpha\sin\beta & \sin\alpha\cos\beta & 0 \end{pmatrix}, \tag{5}$$

where α and β are the spherical coordinates of the nuclear field. Depending on the value of $f(t)$, the solution to the precession equation in between field switchings is

$$\boldsymbol{S}(t) = e^{\boldsymbol{\Omega}t} \cdot \boldsymbol{S}_0, \quad \boldsymbol{S}(t) = e^{-\boldsymbol{\Omega}t} \cdot \boldsymbol{S}_0, \tag{6}$$

where $\boldsymbol{S}_0$ is the initial spin vector.

The time evolution of the spin ensemble can be computed by the theory of continuous-time random walks [23–30]. The difficulty of the theory is reduced since the field modulates between only two values [31,32]. The polarization function is a result of random walks between the two spin environments,

$$\mathbf{P}(t) = \frac{1}{2}\Bigg[e^{\boldsymbol{\Omega}t}\Phi_n(t) + \int_0^t \Phi_0(t-t')e^{-\boldsymbol{\Omega}(t-t')}\Psi_{n0}(t')e^{\boldsymbol{\Omega}t'}dt'$$
$$+ \int_0^t\int_0^{t'} \Phi_n(t-t')e^{\boldsymbol{\Omega}(t-t')}\Psi_{0n}(t'-t'')$$
$$\times e^{-\boldsymbol{\Omega}(t'-t'')}\Psi_{n0}(t'')e^{\boldsymbol{\Omega}t''}dt''dt'$$
$$+ \cdots + \text{signs of } \boldsymbol{\Omega} \text{ switched and } n \leftrightarrow 0\Bigg] \cdot \boldsymbol{S}_0,$$

where Ψ_{ij} are wait-time distributions to transition between state i to state j, and Φ_i are the survival probabilities in state i. Using exponential wait-time distributions leads to

$$\boldsymbol{P}(t) = \frac{1}{2}\Bigg[e^{(\boldsymbol{\Omega}-k_n)t} + \int_0^t e^{(-\boldsymbol{\Omega}-k_0)(t-t')}k_n e^{(\boldsymbol{\Omega}-k_n)t'}dt'$$
$$+ \int_0^t\int_0^{t'} e^{(\boldsymbol{\Omega}-k_n)(t-t')}k_0 e^{(-\boldsymbol{\Omega}-k_0)(t'-t'')}k_n e^{(\boldsymbol{\Omega}-k_n)t''}dt''dt'$$
$$+ \cdots + \text{signs of } \boldsymbol{\Omega} \text{ switched and } n \leftrightarrow 0\Bigg] \cdot \boldsymbol{S}_0. \tag{7}$$

Utilizing the Laplace transform and its convolution properties, the polarization function in the Laplace domain simplifies to

$$\tilde{\boldsymbol{P}}(s) = \frac{1}{2}[(\tilde{\mathbf{R}}_0 + \tilde{\mathbf{R}}_n + (k_0 + k_n)\tilde{\mathbf{R}}_0\tilde{\mathbf{R}}_n)]\sum_{j=0}^{\infty}(k_0k_n\tilde{\mathbf{R}}_0\tilde{\mathbf{R}}_n)^j \cdot \boldsymbol{S}_0, \tag{8}$$

with

$$\tilde{\mathbf{R}}_{0(n)} = \frac{1}{s + k_{0(n)} \pm \boldsymbol{\Omega}}, \tag{9}$$

which has a Laplace transform equal to

$$\tilde{\boldsymbol{P}}(s) = \frac{s + k_0 + k_n}{s(s + k_0 + k_n) - \mathbf{A}} \cdot \boldsymbol{S}_0 = \tilde{\mathbf{M}}(s) \cdot \boldsymbol{S}_0, \tag{10}$$

where

$$\mathbf{A} = -(k_n - k_0)\boldsymbol{\Omega} + \boldsymbol{\Omega}\boldsymbol{\Omega}. \tag{11}$$

This general expression can be analytically transformed to the time domain [33].

We now apply the approximation of fast transitions, $k_{0,n} \gg \gamma B_n$. To leading order in s, $\tilde{\mathbf{M}}(s) = [s\mathbb{1} - \mathbf{A}/(k_0 + k_n)]^{-1}$, which is inverted to be $\mathbf{M}(t) = e^{\mathbf{A}t/(k_0+k_n)}$ and then $\dot{\boldsymbol{P}}(t) = \frac{\mathbf{A}}{k_0+k_n}\boldsymbol{P}(t)$. The next order correction yields [33]

$$\dot{\boldsymbol{P}}(t) = \left(\frac{\mathbf{A}}{k_0 + k_n} - \frac{\mathbf{A}\mathbf{A}}{(k_0 + k_n)^3}\right)\boldsymbol{P}(t), \tag{12}$$

which when written out to second order in $\boldsymbol{\Omega}$ becomes

$$\frac{d\boldsymbol{P}(t)}{dt} = -\frac{1}{4}\frac{\gamma^2}{k_0 + k_n}\left[1 - \left(\frac{k_n - k_0}{k_0 + k_n}\right)^2\right]\boldsymbol{b}_n \times [\boldsymbol{P}(t) \times \boldsymbol{b}_n] - \frac{\gamma}{2}\frac{k_n - k_0}{k_0 + k_n}\boldsymbol{b}_n \times \boldsymbol{P}(t). \tag{13}$$

Only the first term has the capability to relax the spin ensemble. The second term is a correction to the Larmor precession.

By combining spin effects such as spin injection, other spin relaxation sources, and adding back in the applied and average nuclear field in Eq. (3), we can write the following equation to encompass the (nondiffusive) spin evolution,

$$\frac{d\boldsymbol{P}(t)}{dt} = \gamma\left[\boldsymbol{B}_0 + \frac{k_0}{k_0 + k_n}\boldsymbol{b}_n\right] \times \boldsymbol{P}(t) - \frac{1}{\tau_s}\boldsymbol{P}(t) - \gamma^2\tau\boldsymbol{b}_n \times [\boldsymbol{P}(t) \times \boldsymbol{b}_n] + \boldsymbol{G}, \tag{14}$$

where

$$\tau = \frac{1}{4}\frac{1}{k_0 + k_n}\left[1 - \left(\frac{k_n - k_0}{k_0 + k_n}\right)^2\right]. \tag{15}$$

$\boldsymbol{G}||\hat{x}$ is the spin generation vector, and τ_s is due to other spin relaxation mechanisms, which we assume to be isotropic. We have simulated the spin evolution with a Monte Carlo approach and found agreement with solutions to the differential equation (14) [33].

Experiment. To test the theory, we probed the spin polarization $\mathbf{P}$ in n-GaAs using electrical Hanle measurements in a standard three-terminal (3T) configuration. The sample used was an epitaxially grown Co_2MnSi/n-GaAs (100) heterostructure. A 2.5 μm thick Si-doped $n = 4 \times 10^{16}$ cm^{-3} n-GaAs channel was grown on a semi-insulating GaAs (100) substrate. To thin the naturally occurring Schottky barrier and create a tunnel barrier for efficient spin injection [34], a 15 nm $n \rightarrow n^+$ transition layer ($n = 5 \times 10^{18}$ cm^{-3}) was grown, followed by a 18 nm n^+ layer. Then, 5 nm of ferromagnetic (FM) Heusler alloy Co_2MnSi was grown, followed by Al and Au capping layers.

The structures were patterned into lateral spin injection devices [35] using standard photolithographic techniques. The injection contact was 5 μm $\times$ 50 μm. Spin was electrically injected into the n-GaAs channel by imposing a dc current bias (800 A/cm^2 at 0.51 V) across the FM/n-GaAs interface. For the measurements discussed here, the interface was forward biased, so that electrons flowed from the semiconductor into the ferromagnet. In a 3T measurement the FM/n-GaAs interface voltage is measured by measuring the voltage with respect to a remote contact outside of the charge current path. The spin polarization in the channel directly below the injection contact was probed by measuring the change in the 3T voltage ΔV_{3T} upon application of an external out-of-plane magnetic field B. This transverse magnetic field serves to precess the spins and destroy the spin polarization in the channel via the Hanle effect [1].

The influence of DNP on the spin polarization in our samples is most clearly seen by measuring the 3T Hanle effect when the applied field is tilted at small oblique angles θ away from the vertical direction and toward the easy axis of the ferromagnetic contact, as shown in Fig. 1(c). The oblique geometry allows for a significant hyperpolarization of the nuclei (Overhauser effect). Satellite peaks are then observed that correspond to fields at which the applied dephasing transverse field is partially canceled by the Overhauser field [5]. (A less prominent satellite peak at very low fields is due to the Knight field of the polarized electrons.) The effectiveness in reproducing the oblique 3T Hanle line shapes therefore serves as a test of the validity of the model used to account for the effects of DNP.

Discussion. Thus far we have only examined the nondiffusive dynamics. However, the importance of spin diffusion on Hanle curves has been well documented [35]. In light of the theory hitherto presented, we write the following spin drift-diffusion equation,

$$\frac{d\boldsymbol{P}(t)}{dt} = \gamma\left[\boldsymbol{B}_0 + \frac{k_0}{k_0 + k_n}\boldsymbol{b}_n\right] \times \boldsymbol{P}(t) - \frac{1}{\tau_s}\boldsymbol{P}(t) - \gamma^2\tau\boldsymbol{b}_n \times [\boldsymbol{P}(t) \times \boldsymbol{b}_n] + \boldsymbol{G} + D_S\nabla^2\boldsymbol{P}(t) + \frac{\boldsymbol{J}}{ne} \cdot \nabla\boldsymbol{P}(t), \tag{16}$$

which is identical to Eq. (14), except for the addition of the last two terms which describe spin diffusion and spin drift.

The physical device geometry was cast into a one-dimensional (1D) finite-element model, where spin may drift and diffuse laterally in the sample plane. The simplification to 1D is appropriate at cryogenic temperatures given the device aspect ratio, where the spin diffusion length in GaAs is larger than the channel thickness. Equation (16) is iterated forward until steady state ($\frac{d\boldsymbol{P}}{dt} = 0$) is reached. The standard form for the Overhauser field [5] is used to calculate $\boldsymbol{b}_n$ at each spatial coordinate. Upon solving for the steady-state spatially dependent spin polarization in the channel at each applied field, the 3T Hanle signal ΔV_{3T} is extracted by projecting the spin polarization at the injector contact $\boldsymbol{P}_{\text{inj}}$ onto the magnetization of the injector ferromagnet $\boldsymbol{M}$ [1], i.e., $\Delta V_{3T} \propto \boldsymbol{P}_{\text{inj}} \cdot \boldsymbol{M}$. A single overall scaling factor is applied to compare the model to the data.

In Fig. 2, the results of measuring the oblique angle dependence of the 3T Hanle signal at 60 K are shown, along with the corresponding fits to the model described above. For comparison, the effects of adding the anisotropic hyperfine relaxation terms discussed previously are shown side by side with the

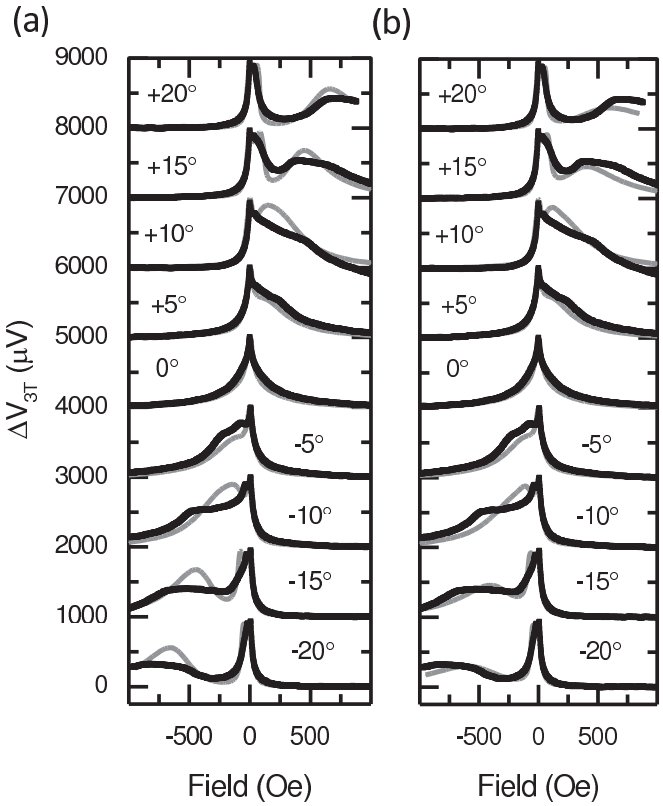

FIG. 2. Shown is the oblique-angle 3T Hanle signal measured at 60 K. The black lines are the experimental data, with a second order (magnetoresistance) background removed and the different angles artificially offset. Shown in gray is the numerical solution to Eq. (16) for the device geometry (a) without the anisotropic hyperfine relaxation terms and (b) with the anisotropic hyperfine relaxation terms included. One set of fitting parameters was used to simultaneously fit all the angles. These fitting parameters for both situations are shown in Table I. The anisotropic hyperfine terms improved the fit the most for larger oblique angles.

fits without the anisotropic hyperfine relaxation terms. In both cases, a single set of parameters is used to fit the data at all angles. The results show that adding the anisotropic hyperfine terms noticeably improve the fitting of the Overhauser peak at large oblique angles, for which diffusion alone systematically overestimates the magnitude and underestimates the width of the satellite peak. Without anisotropic relaxation, the height and width of the satellite are determined only by the spatial variation of the Overhauser field on the scale of the electron spin diffusion length. This mechanism alone, however, is not sufficient to explain the broadening and suppression at larger oblique angles. Inclusion of the additional smaller length-scale nuclear field inhomogeneity, via the anisotropic term, further reduces and broadens the Overhauser peaks. Table I contains the parameters used to fit the 3T signal both without and with the anisotropic hyperfine terms. Note that the addition of the anisotropic mechanism does not change the other fitting parameters significantly, and the isotropic lifetime is essentially unchanged. Measurements were also taken as a function of injection bias current at fixed angle. The fits to the model in this case are comparable to those for the angle

TABLE I. Fitting parameters for curves in Fig. 2.

Parameter	W/o aniso. term	W/ aniso. term
τ_s	3.3 ns	3.4 ns
b_{nuc}	-1.50×10^4 Oe	-1.67×10^4 Oe
b_e	-82 Oe	-73 Oe
$\sqrt{\xi} B_L$	104 Oe	95 Oe
k_0		2.1 ns^{-1}
k_n		0.45 ns^{-1}

dependence at fixed bias. The discrepancy between model and experiment is attributed to a $\pm 1^\circ$ uncertainty in the angle of field with respect to the sample. Additionally, the obtained small values for k_n and k_0 are only on the edge of the strong motional narrowing approximation.

Oblique angles larger than $\pm 20^\circ$ were experimentally inaccessible due to the switching of the ferromagnetic contact when the in-plane component of the field reached the coercive field. Figure 3 shows the solutions of Eq. (16) for two larger angles, 30° and 45°. The trend followed at these higher angles is similar to what is viewed at the lower ones—the anisotropic terms tend to decrease the magnitude of the Overhauser peak (black) when compared to their exclusion (red). If ferromagnetic contacts with larger coercivity are available, a more rigorous test of the predictions of this theory will be possible.

Now, we consider how the anisotropic mechanism may also be evident in optical spin injection experiments [7,8,19]. In these experiments, the nuclear field is extracted by taking the difference of the total precession frequency and the precession frequency due solely to the applied field [22]. As we have discussed here, due to the inherent inhomogeneity of the nuclear field, the inferred nuclear field is actually an *average* nuclear field in the probed macroscopic optical spot size. From Eq. (14), the inferred nuclear field is then $\overline{\boldsymbol{B}_n} = k_0 \boldsymbol{b}_n/(k_0 + k_n)$, which leads to the anisotropic term

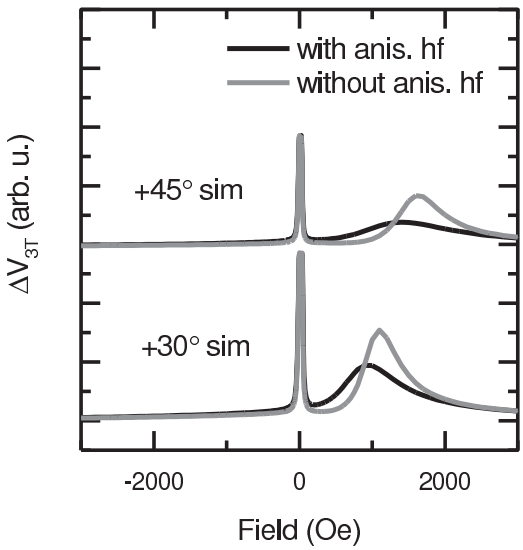

FIG. 3. Large angle solutions to the spin diffusion model, Eq. (16), with and without the anisotropic spin relaxation terms.

being

$$-\gamma^2 \frac{(k_0 + k_n)^2}{k_0^2} \tau \overline{\boldsymbol{B}_n} \times [\boldsymbol{P}(t) \times \overline{\boldsymbol{B}_n}]. \quad (17)$$

We predict this term to be observable in time-resolved Faraday or Kerr rotation experiments.

Conclusions. The influence of DNP on spin evolution in semiconductors has been observed for many years. However, the inherent inhomogeneity of the large nuclear fields has been neglected as a spin relaxation process. We have shown that the nuclear field inhomogeneity leads to an anisotropic spin relaxation mechanism and we have demonstrated that this mechanism can account for the oblique Hanle measurements of electrical spin injection into n-GaAs.

Acknowledgments. This work was supported in part by C-SPIN, one of six centers of STARnet, a Semiconductor Research Corporation program, sponsored by MARCO and DARPA, and by NSF under DMR-1104951.

[1] X. Lou, C. Adelmann, M. Furis, S. A. Crooker, C. J. Palmstrøm, and P. A. Crowell, Phys. Rev. Lett. **96**, 176603 (2006).
[2] P. A. Crowell and S. A. Crooker, in *Handbook of Spin Transport and Magnetism*, edited by E. Y. Tysmbal and I. Zutic (CRC Press, Boca Raton, FL, 2012), Chap. 23, p. 463.
[3] C. Awo-Affouda, O. M. J. van 't Erve, G. Kioseoglou, A. T. Hanbicki, M. Holub, C. H. Li, and B. T. Jonker, Appl. Phys. Lett. **94**, 102511 (2009).
[4] G. Salis, A. Fuhrer, and S. F. Alvarado, Phys. Rev. B **80**, 115332 (2009).
[5] M. K. Chan, Q. O. Hu, J. Zhang, T. Kondo, C. J. Palmstrøm, and P. A. Crowell, Phys. Rev. B **80**, 161206(R) (2009).
[6] D. Paget, G. Lampel, B. Sapoval, and V. I. Safarov, Phys. Rev. B **15**, 5780 (1977).
[7] F. Meier and B. P. Zachachrenya, *Optical Orientation: Modern Problems in Condensed Matter Science* (North-Holland, Amsterdam, 1984), Vol. 8.
[8] J. M. Kikkawa and D. D. Awschalom, Science **287**, 473 (2000).
[9] G. Salis, Y. Kato, K. Ensslin, D. C. Driscoll, A. C. Gossard, and D. D. Awschalom, Nature (London) **414**, 619 (2001).
[10] A. L. Falk, P. V. Klimov, V. Ivády, K. Szász, D. J. Christle, W. F. Koehl, A. Gali, and D. D. Awschalom, Phys. Rev. Lett. **114**, 247603 (2015).
[11] J. Huang, Y. S. Chen, A. Ludwig, D. Reuter, A. D. Wieck, and G. Bacher, Appl. Phys. Lett. **100**, 132103 (2012).
[12] K. D. Christie, C. C. Geppert, S. J. Patel, Q. O. Hu, C. J. Palmstrøm, and P. A. Crowell, arXiv:1406.0436.
[13] M. E. Flatté and J. M. Byers, Phys. Rev. Lett. **84**, 4220 (2000).
[14] *Semiconductor Spintronics and Quantum Computation*, edited by D. D. Awschalom, N. Samarth, and D. Loss (Springer, Heidelberg, 2002).
[15] Z. G. Yu and M. E. Flatté, Phys. Rev. B **66**, 235302 (2002).
[16] S. A. Crooker and D. L. Smith, Phys. Rev. Lett. **94**, 236601 (2005).
[17] S. A. Crooker, M. Furis, X. Lou, C. Adelmann, D. L. Smith, C. J. Palmstrøm, and P. A. Crowell, Science **309**, 2191 (2005).
[18] Y. K. Kato, R. C. Myers, A. C. Gossard, and D. D. Awschalom, Appl. Phys. Lett. **86**, 162107 (2005).
[19] Y.-S. Ou, Y.-H. Chiu, N. J. Harmon, P. Odenthal, M. Sheffield, M. Chilcote, R. K. Kawakami, M. E. Flatté, and E. Johnston-Halperin, arXiv:1508.00164.
[20] D. Kölbl, D. M. Zumbühl, A. Fuhrer, G. Salis, and S. F. Alvarado, Phys. Rev. Lett. **109**, 086601 (2012).
[21] J. Stephens, J. Berezovsky, J. P. McGuire, L. J. Sham, A. C. Gossard, and D. D. Awschalom, Phys. Rev. Lett. **93**, 097602 (2004).
[22] R. Kawakami, Y. Kato, M. Hanson, I. Malajovich, J. Stephens, E. Johnston-Halperin, G. Salis, A. Gossard, and D. Awschalom, Science **294**, 131 (2001).
[23] E. W. Montroll and G. H. Weiss, J. Math. Phys. **6**, 167 (1965).
[24] H. Scher and M. Lax, Phys. Rev. B **7**, 4491 (1973).
[25] K. W. Kehr, G. Honig, and D. Richter, Z. Phys. B **32**, 49 (1978).
[26] R. S. Hayano, Y. J. Uemura, J. Imazato, N. Nishida, T. Yamazaki, and R. Kubo, Phys. Rev. B **20**, 850 (1979).
[27] R. Czech, J. Chem. Phys. **91**, 2506 (1989).
[28] N. J. Harmon and M. E. Flatté, Phys. Rev. Lett. **110**, 176602 (2013).
[29] N. J. Harmon and M. E. Flatté, Phys. Rev. B **90**, 115203 (2014).
[30] A. Yaouanc and P. D. de Rèotier, *Muon Spin Rotation, Relaxation, and Resonance* (Oxford University Press, New York, 2011).
[31] P. Borgs, K. W. Kehr, and P. Heitjans, Phys. Lett. A **155**, 429 (1991).
[32] P. Borgs, K. W. Kehr, and P. Heitjans, Phys. Rev. B **52**, 6668 (1995).
[33] See Supplemental Material at http://link.aps.org/supplemental/10.1103/PhysRevB.92.140201 for analytic solution to the inverse Laplace transform of Eq. (10), estimation of second order damping term given in Eq. (12), and a comparison of solutions in text with Monte Carlo simulations.
[34] A. T. Hanbicki, O. M. J. Van't Erve, R. Magno, G. Kioseoglou, C. H. Li, B. T. Jonker, G. Itskos, R. Mallory, M. Yasar, and A. Petrou, Appl. Phys. Lett. **82**, 4092 (2003).
[35] X. Lou, C. Adelmann, S. A. Crooker, E. S. Garlid, J. Zhang, K. S. M. Reddy, S. D. Flexner, C. J. Palmstrøm, and P. A. Crowell, Nat. Phys. **3**, 197 (2007).